Template Synthesis of Nanotubes by Room-Temperature Coalescence of Metal Nanoparticles

Tali Sehayek, Michal Lahav, Ronit Popovitz-Biro, Alexander Vaskevich, and Israel Rubinstein*

Department of Materials and Interfaces, Weizmann Institute of Science, Rehovot 76100, Israel

Received January 17, 2005. Revised Manuscript Received April 28, 2005

Metal nanoparticle nanotubes (NPNTs) have been introduced by us as a new class of template-synthesized, nanoparticle-based nanotubes possessing unique features such as room-temperature preparation, highly corrugated wall structure, electrical conductivity, mechanical stability, and defined optical absorbance. The nanotubes are prepared by passing a citrate-stabilized metal (Au, Ag) colloid solution through the pores of an aminosilane-modified nanoporous alumina membrane. The nanoparticles (NPs) aggregate, forming multilayers on the pore walls, and undergo spontaneous room-temperature coalescence to afford solid, porous, multiwall metallic nanotubes. Self-sustained NPNTs are obtained by membrane dissolution. It is shown that the nanotubes are formed in two stages, i.e., NP accumulation and initial coalescence in the wet stage, and final solidification upon drying, both crucial to their formation. The NPNT synthetic scheme is extended here to the construction of composite NPNTs, i.e., formation of bimetallic Au−Pd NPNTs using a mixed colloid solution. High-resolution transmission electron microscopy (HRTEM) of single-metal and composite NPNTs indicates actual coalescence and creation of metallic interfaces between individual NPs, with lattice continuation that extends into the NP bulk.

Introduction

Nanotubes (NTs) constitute a particularly interesting family of nano-objects. They represent a combination of properties which may be important for various applications, such as nanometer dimensions, elongated geometry, a defined cavity, accessible inner and outer surfaces, and (possible) control of the size, aspect ratio, chemical composition and chirality. There is a large number of publications dealing with NTs of various kinds, including carbon,[1,2] inorganic,[3−6] polymeric[7−9] and metallic NTs. Template synthesis, used by Martin et al.[10−14] and others,[15−28] is the most common scheme for metal NT formation. NTs made of various metals (e.g., Au,[10−14,25,28] Ag,[21,22,25] Pd,[20,25] Pt,[25−27] Ru[23]) or composites (e.g., gold/carbon,[18] platinum/polystyrene,[17] palladium/polystyrene,[16] tin/platinum,[19] ruthenium/platinum[23]) were synthesized using several procedures, all of which involve reduction of metal ions inside the template.

We have recently presented a new kind of metal nanotubes, denoted nanoparticle nanotubes (NPNTs).[29] The NPNTs are prepared by a novel room-temperature process, where colloid solutions containing preformed, citrate-stabilized Au or Ag nanoparticles (NPs) are passed through the pores of an aminosilane-modified nanoporous alumina membrane. The

* Corresponding author. E-mail: israel.rubinstein@weizmann.ac.il. Phone: +972 8 9342678. Fax: +972 8 9344137.

(1) Iijima, S. *Nature* **1991**, *354*, 56.
(2) Ajayan, P. M. *Chem. Rev.* **1999**, *99*, 1787−1799.
(3) Tenne, R. *Angew. Chem., Int. Ed. Engl.* **2003**, *42*, 5124−5132.
(4) Leontidis, E.; Orphanou, M.; Kyprianidou-Leodidou, T.; Krumeich, F.; Caseri, W. *Nano Lett.* **2003**, *3*, 569−572.
(5) Rao, C. N. R.; Nath, M. *Dalton Trans.* **2003**, *1*, 1−25.
(6) Caruso, R. A.; Schattka, J. H.; Greiner, A. *Adv. Mater.* **2001**, *13*, 1577−1579.
(7) Feng, L.; Li, S. H.; Li, H. J.; Zhai, J.; Song, Y. L.; Jiang, L.; Zhu, D. B. *Angew. Chem., Int. Ed. Engl.* **2002**, *41*, 1221−1223.
(8) Steinhart, M.; Wendorff, J. H.; Greiner, A.; Wehrspohn, R. B.; Nielsch, K.; Schilling, J.; Choi, J.; Gosele, U. *Science* **2002**, *296*, 1997−1997.
(9) Liang, Z. J.; Susha, A. S.; Yu, A. M.; Caruso, F. *Adv. Mater.* **2003**, *15*, 1849−1853.
(10) Martin, C. R.; Mitchell, D. T. In *Electroanalytical Chemistry*; Bard, A. J., Rubinstein, I., Eds.; Marcel Dekker: New York, 1999; Vol. 21, pp 1−74.
(11) Kohli, P.; Wharton, J. E.; Braide, O.; Martin, C. R. *J. Nanosci. Nanotechnol.* **2004**, *4*, 605−610.
(12) Hulteen, J. C.; Martin, C. R. *J. Mater. Chem.* **1997**, *7*, 1075−1087.
(13) Wirtz, M.; Parker, M.; Kobayashi, Y.; Martin, C. R. *Chem.-Eur. J.* **2002**, *8*, 3573−3578.
(14) Martin, C. R. *Science* **1994**, *266*, 1961−1966.
(15) Steinhart, M.; Wehrspohn, R. B.; Gosele, U.; Wendorff, J. H. *Angew. Chem., Int. Ed. Engl.* **2004**, *43*, 1334−1344.
(16) Steinhart, M.; Wendorff, J. H.; Wehrspohne, R. B. *ChemPhysChem* **2003**, *4*, 1171−1176.
(17) Luo, Y.; Lee, S. K.; Hofmeister, H.; Steinhart, M.; Gosele, U. *Nano Lett.* **2004**, *4*, 143−147.
(18) Goring, P.; Pippel, E.; Hofmeister, H.; Wehrspohn, R. B.; Steinhart, M.; Gosele, U. *Nano Lett.* **2004**, *4*, 1121−1125.
(19) Guo, Y. G.; Hu, J. S.; Zhang, H. M.; Liang, H. P.; Wan, L. J.; Bai, C. L. *Adv. Mater.* **2005**, *17*, 746−750.
(20) Steinhart, M.; Jia, Z. H.; Schaper, A. K.; Wehrspohn, R. B.; Gosele, U.; Wendorff, J. H. *Adv. Mater.* **2003**, *15*, 706−709.
(21) Park, J. H.; Oh, S. G.; Jo, B. W. *Mater. Chem. Phys.* **2004**, *87*, 301−310.
(22) Qu, L. T.; Shi, G. Q.; Wu, X. F.; Fan, B. *Adv. Mater.* **2004**, *16*, 1200−1203.
(23) Chen, J.; Tao, Z. L.; Li, S. L. *J. Am. Chem. Soc.* **2004**, *126*, 3060−3061.
(24) Sanchez-Castillo, M. A.; Couto, C.; Kim, W. B.; Dumesic, J. A. *Angew. Chem., Int. Ed. Engl.* **2004**, *43*, 1140−1142.
(25) Kijima, T.; Yoshimura, T.; Uota, M.; Ikeda, T.; Fujikawa, D.; Mouri, S.; Uoyama, S. *Angew. Chem., Int. Ed. Engl* **2004**, *43*, 228−232.
(26) Yoo, W. C.; Lee, J. K. *Adv. Mater.* **2004**, *16*, 1097−1101.
(27) Zhao, Y.; Guo, Y. G.; Zhang, Y. L.; Jiao, K. *Phys. Chem. Chem. Phys.* **2004**, *6*, 1766−1768.
(28) Demoustier-Champagne, S.; Delvaux, M. *Mater. Sci. Eng. C−Biomimetic Supramol. Syst.* **2001**, *15*, 269−271.
(29) Lahav, M.; Sehayek, T.; Vaskevich, A.; Rubinstein, I. *Angew. Chem., Int. Ed. Engl.* **2003**, *42*, 5575−5579.

10.1021/cm0501057 CCC: $30.25 © 2005 American Chemical Society
Published on Web 06/08/2005

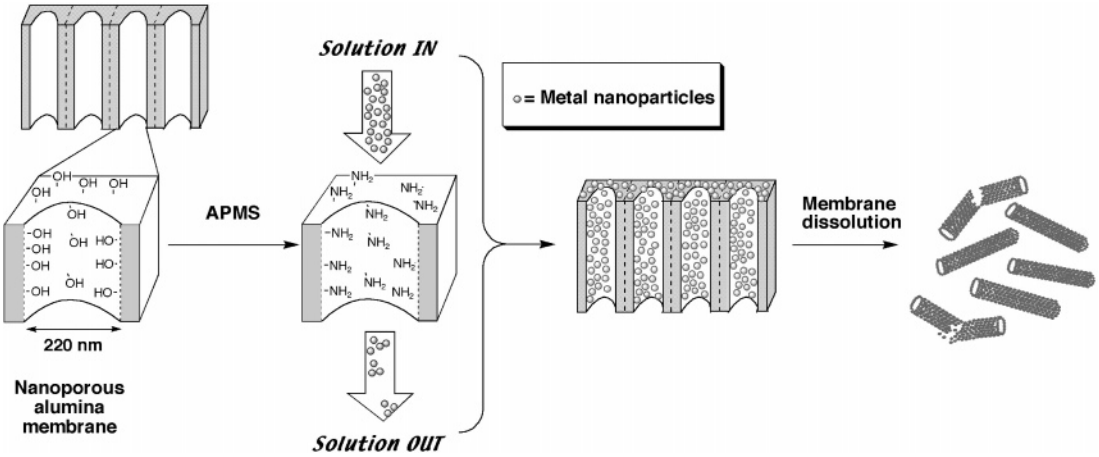

Figure 1. Schematic diagram showing the preparation of metal NPNTs: A nanoporous alumina membrane is first silanized. A nanoparticle solution is then passed through the silanized alumina membrane, followed by washing, drying, and (optional) membrane dissolution (dimensions are not to scale).

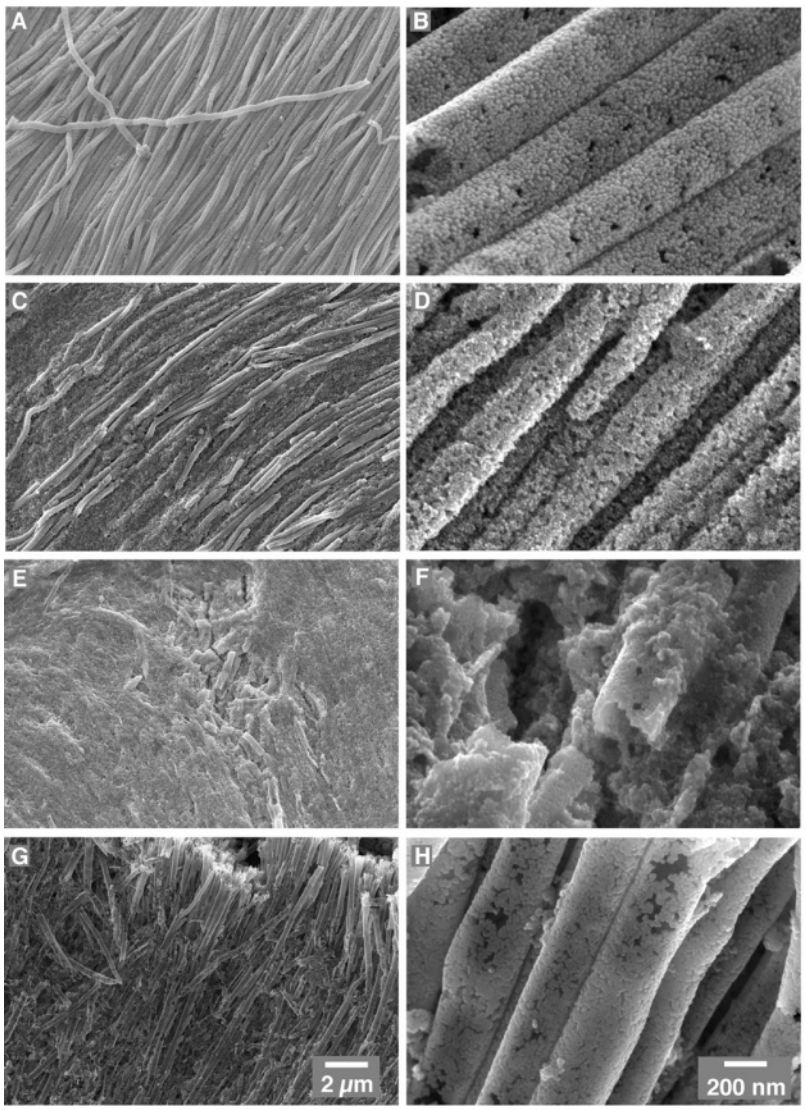

Figure 2. (A−D) HRSEM images of Au NPNTs obtained after passing Au NP solution, followed by (A, B) drying or (C, D) no drying prior to membrane dissolution (different magnifications are shown). (E−H) HRSEM images (different magnifications) of Pd NP structures obtained by applying the usual NPNT preparation procedure; (G, H) sample annealed (350 °C, 17 h) prior to alumina membrane dissolution.

NPs bind to the pore walls, aggregate into multilayer structures (see Figure 2d in ref 29), and spontaneously coalesce to form solid, porous, nanoparticle-based nanotubes. The latter can be obtained as self-sustained NPNTs by dissolution of the membrane template. The Au NPNTs were shown to be mechanically stable and electrically conducting and display a characteristic surface plasmon optical absorbance.

The unique procedure of NPNT formation, i.e., room-temperature coalescence of metal NPs, provides substantial variability, enabling use of metal NPs of different sizes and compositions, as well as mixtures of NPs, to obtain special properties. The formation of complex structures is exemplified here by the construction of composite Au−Pd NPNTs. The inclusion of Pd NPs is of particular interest for applications such as catalysis or hydrogen sensing.[30−33]

The mechanism of the spontaneous, room-temperature coalescence of metal NPs to form solid NTs is shown here to involve NP accumulation on the pore walls and initial coalescence during colloid flow through the membrane, and final coalescence in the drying step. The nature of the interface between adjacent NPs in single-metal and bimetallic NPNTs is revealed by high-resolution transmission electron microscopy (HRTEM), showing NP coalescence and lattice continuation at the interfaces.

Experimental Section

Chemicals. $HAuCl_4*3H_2O$ was prepared according to a known procedure.[34] Tri-sodium citrate dihydrate (Merck), potassium hexachloropalladate (IV) (Aldrich), NaOH (Merck), 3-aminopropyl trimethoxysilane (APMS) (Aldrich), 2-propanol (Biolab), H_2SO_4 (95−98%, Palacid), and H_2O_2 (30%, Frutarom), were used as received. Alumina membranes (0.2 μm, Anodisc, Whatman) were sonicated in 2-propanol prior to use. Water was triply distilled. Household nitrogen (>99%, from liquid nitrogen) was used for drying the samples. All glassware and Teflonware were treated with Piranha solution (boiling H_2SO_4:H_2O_2, 2:1 by volume), followed by rinsing with deionized water and triply distilled water. (Caution: Piranha solution reacts violently with organic materials and should be handled with extreme care.)

Nanoparticle Preparation. Au NPs (14±2 nm average core diameter, citrate stabilized) were synthesized according to a literature procedure,[35] multiplying the original concentrations by five. Pd NPs (14±2 nm average core diameter, citrate stabilized) were synthesized according to a literature procedure,[36] multiplying the original concentrations by 4.5. Mixed Au−Pd NP solutions (50:50 atomic %) were obtained by mixing the single-metal NP solutions.

Nanoparticle Nanotube (NPNT) Preparation. Nanoporous alumina membranes were modified with APMS,[37] resulting in amino-derivatized pore walls. A 18 mL sample of Au, Pd or Au−Pd NP solution was passed through the membrane pores by vacuum suction using the following protocol: (i) Passing 10 mL of the NP solution through the membrane. (ii) Sonicating the membrane for 4 min. (iii) Passing a few mL of triply distilled water through the membrane. (iv) Passing additional 8 mL of NP solution. (v) Washing by passing distilled water through the pores (indicating that the membrane is not blocked). Unless otherwise specified, the membranes were then dried under a stream of nitrogen. To achieve self-sustained NPNTs the alumina membrane was dissolved using 1.0 M NaOH for 2.5 h followed by washing with triply distilled water. The entire process of NPNT formation was carried out at room temperature, corresponding to 22−23 °C.

Electron Microscopy. High-resolution scanning electron microscope (HRSEM) secondary electron (SE) imaging was carried out with a LEO−Supra 55 VP HRSEM, using an in-lens detector. Membrane dissolution for SEM imaging was carried out on the stub. Elemental analysis was carried out with a Philips XL30 ESEM-FEG microscope, using the energy dispersive spectrophotometer (EDS). High-resolution transmission electron microscopy (HRTEM) and elemental mapping by energy filtered transmission electron microscopy (EFTEM) were performed with a Tecnai F30−UT (FEI) microscope (300 kV, field emission gun), equipped with a GIF (Gatan Imaging Filter). Images were acquired using a Gatan 1kx1k CCD camera and image processing was performed by Digital Micrograph software. Samples for HRTEM imaging were prepared as follows: A NPNT solution was obtained by dissolving a colloid-treated alumina membrane in 1.0 M NaOH, followed by removal of the solution and redispersion of the NPNTs in pure water. A NPNT or NP solution was evaporated on a carbon coated TEM Cu grid (400 mesh) for imaging. Specimens for palladium mapping by EFTEM were places on holey carbon films (Quantifoil), to reduce the strong tail of the carbon edge, which interferes with the background subtraction routine.

Results and Discussion

Preparation of Nanoparticle Nanotubes (NPNTs). The NPNT preparation scheme[29] is shown in Figure 1. A nanoporous alumina membrane (220 nm average pore diameter) is modified with APMS, resulting in amino-derivatized pore walls. An aqueous citrate-stabilized metal colloid solution is passed through the modified membrane pores by vacuum suction. The NPs bind to the exposed amine groups, aggregate, and form NP multilayers on the pore walls, followed by spontaneous, room-temperature coalescence to produce solid tubes. The membrane template can be dissolved (in 1.0 M NaOH) to obtain self-sustained, porous, multiwall tubular structures (NPNTs).

Gold NPNTs. Figure 2A,B shows high-resolution scanning electron microscope (HRSEM) images of free-standing Au NPNTs, obtained after passing the colloid solution (14 nm average Au core diameter) through the membrane, followed by washing, drying, and membrane dissolution. The first NP layer is formed by binding of citrate-stabilized NPs to the amine groups on the pore walls. It is assumed that partial stripping of the citrate stabilizing shell on the NPs is the driving force for further NP immobilization and multilayer formation in the pores, while the final stages of coalescence are promoted by membrane drying. The latter is evident in Figure 2C,D, showing HRSEM images of the structure obtained by carrying out the same procedure without drying the membrane prior to its dissolution, resulting in poorly defined tubular structures. Moreover, a membrane stored in water for a month after passing the NP solution, followed by template dissolution, showed the same result as that presented in Figure 2C,D, indicating that the final nanotube coalescence and solidification occur in the drying step.

(30) Kobayashi, J.; Mori, Y.; Okamoto, K.; Akiyama, R.; Ueno, M.; Kitamori, T.; Kobayashi, S. *Science* **2004**, *304*, 1305−1308.
(31) Shen, Y.; Bi, L. H.; Liu, B. F.; Dong, S. J. *New J. Chem.* **2003**, *27*, 938−941.
(32) Lahtinen, R.; Johans, C.; Hakkarainen, S.; Coleman, D.; Kontturi, K. *Electrochem. Commun.* **2002**, *4*, 479−482.
(33) Fukuoka, A.; Araki, H.; Sakamoto, Y.; Inagaki, S.; Fukushima, Y.; Ichikawa, M. *Inorg. Chim. Acta* **2003**, *350*, 371−378.
(34) Block, B. P. *Gold Powder and Potassium Tetrabromoaurate(III)*; McGraw-Hill Book Co., New York, 1953; Vol. 4.
(35) Turkevich, J.; Stevenson, P. C.; Hiller, J. *Discuss. Faraday Soc.* **1951**, *11*, 55−75.
(36) Dokoutchaev, A.; James, J. T.; Koene, S. C.; Pathak, S.; Prakash, G. K. S.; Thompson, M. E. *Chem. Mater.* **1999**, *11*, 2389−2399.
(37) Goss, C. A.; Charych, D. H.; Majda, M. *Anal. Chem.* **1991**, *63*, 85−88.

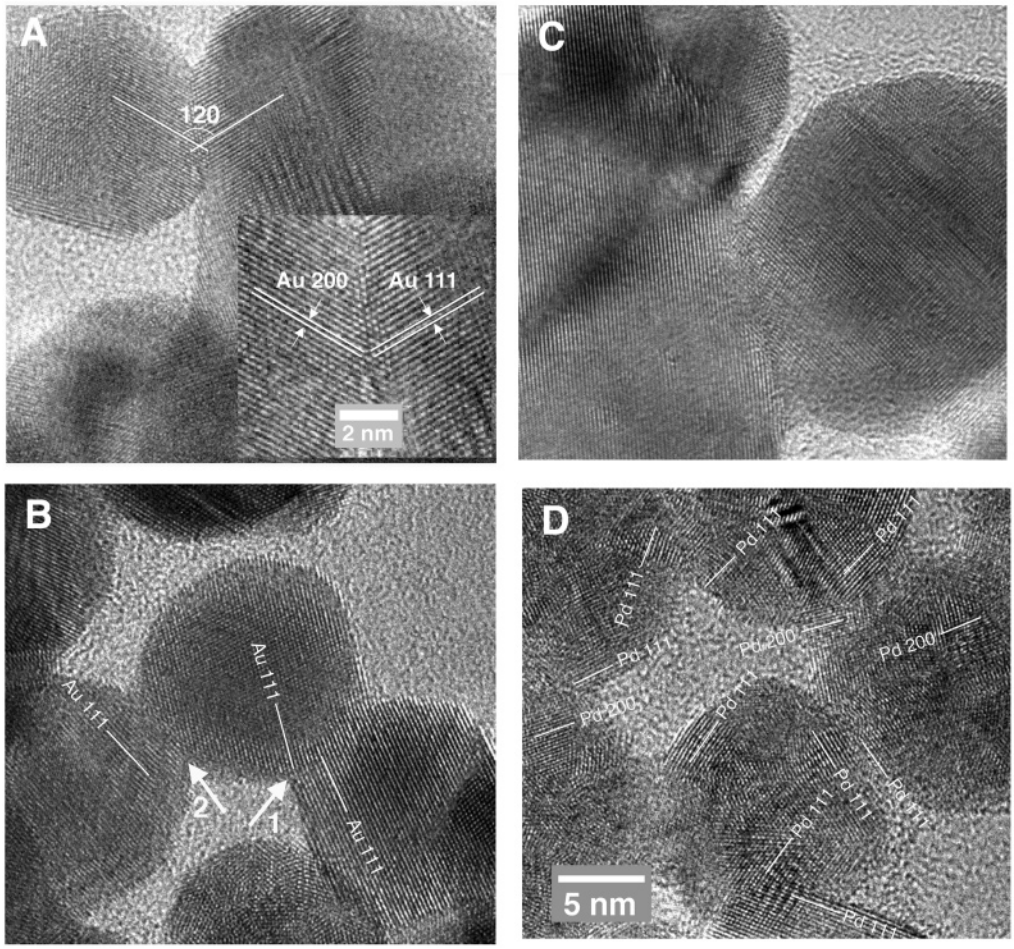

Figure 3. HRTEM images showing Au (A−C) and Pd (D) NP aggregates obtained by applying a drop of NPNT (A, B, D) or NP (C) solution on a carbon-coated TEM grid. In all cases formation of metallic interfaces with lattice continuation is seen. Lattice planes in A, B, and D emerge from the drawn lines, perpendicular to the image plane.

The nature of the interface between adjacent metal NPs in the final NPNTs is of particular interest, as it determines the NPNT properties and provides information on the mechanism of NPNT formation. A characteristic HRTEM image highlighting the interface between Au NPs in a NPNT is shown in Figure 3A. The image shows full coalescence and metallic interfaces between the NPs, with continuation of lattice planes. Several points should be emphasized: (i) Different lattice planes are involved in the coalescence, with no preferred orientation (Figure 3A). (ii) In most cases, good registry of lattice planes across the interface is observed, with clear lattice continuation; however, in some cases, lattice continuation is not seen. Both situations are demonstrated in Figure 3B: The interface marked **1** shows order and lattice continuation, while the interface marked **2** appears less ordered, possibly representing a ripening situation. Note that in most cases where lattice continuation is observed across the NP−NP interface, the lattice matching extends well beyond the interface region into the NP bulk. This raises an interesting mechanistic question, i.e., whether lattice continuation is attained by NP rotation prior to coalescence, or by lattice rearrangement during/after coalescence. This issue has yet to be resolved.

The question of whether the process of metal NP room-temperature coalescence upon aggregation and drying is unique to NP accumulation on the membrane pore walls, is addressed in Figure 3C, where a HRTEM image of a drop of Au NP solution, dried on a carbon-coated TEM grid, is shown. The image is reminiscent of those of the NPNTs (Figure 3A,B), showing aggregation and coalescence with lattice continuation. In the case of the dried NP drop, the coalescence appears to be more extensive with noted NP enlargement, presumably due to the more compact NP layer compared with that obtained during aggregation on the membrane walls. The basic process, however, appears similar and not unique to the membrane case.[38−42]

Palladium NPNTs. Formation of Pd NPNTs is of particular interest in light of the various applications of Pd metal (catalysis, hydrogen sensing, etc.). The NPNT preparation scheme was therefore applied to the formation of Pd NPNTs, using citrate-stabilized Pd NPs of 14 nm average core diameter. Similar to Au NPs, the Pd NPs interact with the amine groups on the silanized membrane walls. In the case of Pd, however, after drying and membrane dissolution NPNTs are not obtained, only highly fragile tubular frag-

(38) Alcantar, N. A.; Park, C.; Pan, J. M.; Israelachvili, J. N. *Acta Mater.* **2003**, *51*, 31−47.
(39) Ferguson, G. S.; Chaudhury, M. K.; Sigal, G. B.; Whitesides, G. M. *Science* **1991**, *253*, 776−778.
(40) Tang, Z. Y.; Kotov, N. A.; Giersig, M. *Science* **2002**, *297*, 237−240.
(41) Sra, A. K.; Schaak, R. E. *J. Am. Chem. Soc.* **2004**, *126*, 6667−6672.
(42) Giersig, M.; Pastoriza-Santos, I.; Liz-Marzan, L. M. *J. Mater. Chem.* **2004**, *14*, 607−610.

ments, as seen in the HRSEM images in Figure 2E,F. A HRTEM image showing a Pd NPNT fragment is presented in Figure 3D; despite the absence of free-standing tubes, room-temperature coalescence and formation of metallic interfaces between Pd NPs in the solid fragments is seen. Note that images similar to the one shown in Figure 3D are observed with a Pd colloid solution dried on a TEM grid (not shown).

To understand the difference between the Au (or Ag[29]) and Pd cases, the weight of Au and Pd in the membrane after passing the metal colloid solution, washing (by passing water) and drying, was determined. The results show that the number of Pd NPs accumulated in the membrane during NPNT preparation is ca. 6 times lower than that of Au NPs under similar conditions. This indicates that in the first stage, i.e., passing the colloid solution in the modified membrane, Au NPs aggregate in multilayers and undergo initial coalescence, while in the case of Pd NPs no accumulation occurs beyond the first NP layer bound to the amine-terminated walls. Hence, in the drying step the Au NPs undergo final coalescence to form solid, multiwall NPNTs, whereas in the drying step of the Pd NPs only the first layer of NPs exists and undergoes coalescence. The single-layered Pd tubular structures are mechanically unstable and disintegrate during membrane dissolution. This resembles the initial stages of Au NPNT formation, previously described by us (Figure 4 in ref 29). This assumption is substantiated by obtaining self-sustained, single-wall Pd NPNTs using enhanced coalescence: Annealing of a membrane (17 h at 350 °C) after passing the Pd NP solution, washing, and drying, results in more stable Pd NPNTs. Membrane dissolution shows formation of single-layered Pd tubes (Figure 2G,H), the result of high-temperature sintering of the amine-bound Pd NP monolayer on the pore walls.

It is therefore evident that room-temperature formation of free-standing multilayered NPNTs depends on evolution of the structure by aggregation and coalescence of metal NPs, initiated during the stage of passing the colloid solution. The diffusion coefficient for self-diffusion of Au in the solid state is notably higher than that of Pd: Extrapolation of data[43,44] obtained at 300−600 °C to room temperature gives $\log(D_{Au}, cm^2/s) \approx -17.3$ and $\log(D_{Pd}, cm^2/s) \approx -19.9$. The considerably lower value of D_{Pd} is probably responsible for the decreased probability for sticking of NPs and accumulation of multilayered structures. Another difference between the Au and Pd NPs is their microstructure. Unlike the Au NPs (Figure 3A-C), which are largely monocrystalline, the Pd NPs appear extensively polycrystalline (Figure 3D). However, the effect of the NP crystallinity on the spontaneous coalescence is not yet clear.

Composite NPNTs. The NPNT preparation scheme was applied to the formation of composite, bi-metallic Au−Pd NPNTs, using a mixed solution of citrate-stabilized Au and Pd NPs. Although pure Pd NP solutions do not induce room-temperature formation of self-sustained NPNTs (Figure 2E,F), when mixed with Au NPs the result is high-quality NPNTs, as seen by HRSEM imaging (Figure 4A−C). Energy-dispersive spectroscopy (EDS) of the composite NPNTs (Figure 4D) indicates that the 1:1 ratio (atomic %) of the NPs in solution is preserved in the tubes.

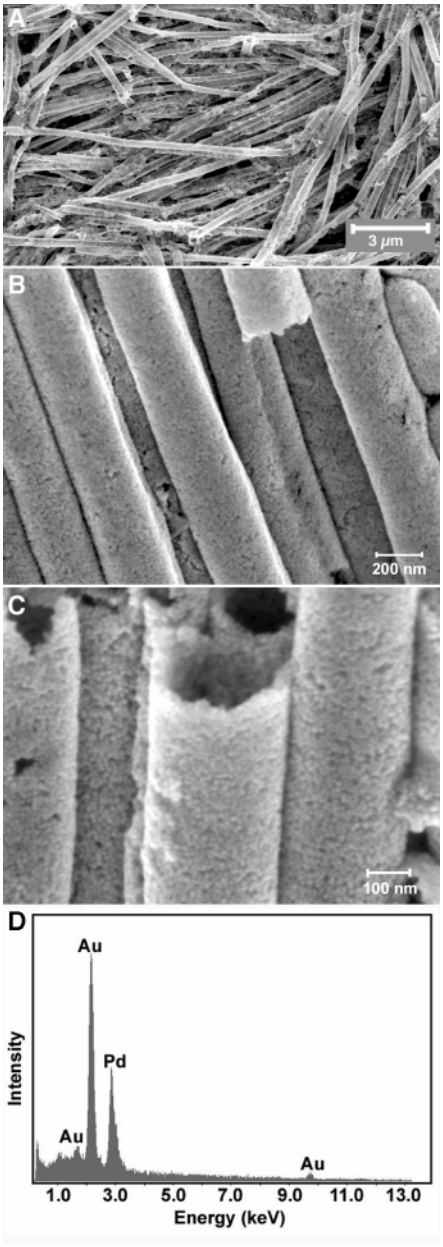

Figure 4. (A−C) HRSEM images of composite Au−Pd NPNTs (1:1) at different magnifications, obtained using a mixed 1:1 (atomic %) Au and Pd NP solution. (D) Energy dispersive spectrum (EDS) of Au−Pd NPNTs, giving an atomic % ratio of 51% Au, 49% Pd.

The distribution of individual Pd and Au NPs in the composite NPNTs was revealed by Pd mapping using energy-filtering TEM (EFTEM). Figure 5A shows a zero-loss image of the NPs in a Au−Pd NPNT fragment, while Figure 5B shows a Pd map of the same fragment, where the Pd NPs appear bright. The latter image suggests that the Au and Pd NPs are not distributed completely randomly, but rather as small aggregates of NPs of the same kind. Figure 5C is a HRTEM image of the area marked in A and B, showing interfaces between Au and Pd NPs. It is clear that the NPs maintain their identity, with effective coalescence

(43) Beszeda, I.; Gontier-Moya, E. G.; Beke, D. L. *Surf. Sci.* **2003**, *547*, 229−238.
(44) Beszeda, I.; Szabo, I. A.; Gontier-Moya, E. G. *Appl. Phys. A* **2004**, *78*, 1079−1084.

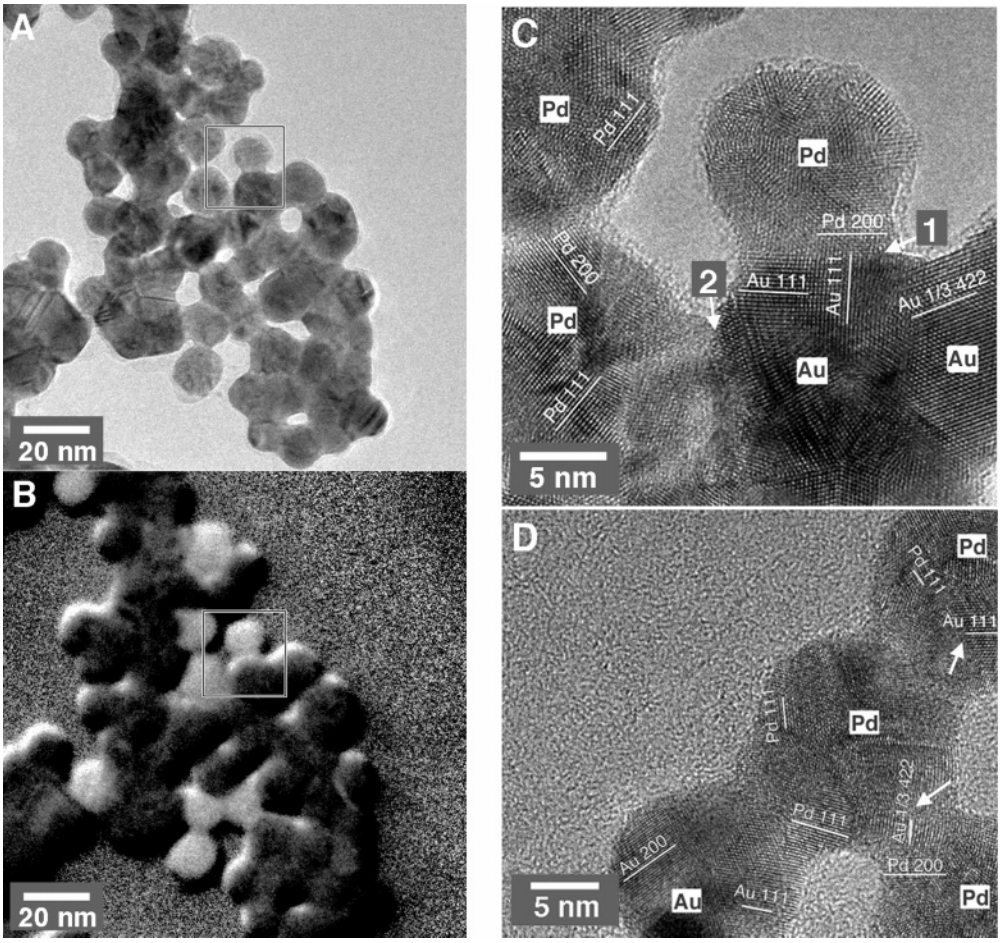

Figure 5. (A) zero-loss TEM image of the NPs in a Au−Pd NPNT fragment. (B) Pd map (385−405 eV) of the same fragment, where Pd NPs appear bright. (C) HRTEM image of the area marked in A and B, showing the Au and Pd NPs (indicated) after coalescence. (D) HRTEM image of another Au−Pd NPNT fragment (Pd mapping not shown); spots with Au d-spacings appearing on Pd NPs are marked with arrows (see text). Lattice planes in C and D emerge from the drawn lines, perpendicular to the image plane.

seen at the Au−Pd interface marked **1** (the interface marked **2** is not clear); the interface appears crystalline with continuation of lattice planes and a rather sharp transformation from one metal to the other. Alloy formation appears to be limited to a few atomic layers at the interface. An interesting situation is seen in Figure 5D, where spots with Au d-spacing appear on Pd NPs (marked with arrows). Such Au spots, seen occasionally in Pd areas, probably represent the remains of Au NPs which were situated above these spots and were disconnected during sample preparation.

Conclusions

It was shown that our NPNT synthetic scheme can be extended to the formation of composite nanotubes comprising two (or more) different metal NPs, where each constituent maintains its chemical identity. This opens the way to the preparation of NPNTs combining the properties of different materials, such as optical, mechanical, electrical, and catalytic, in the same nanotube. HRTEM imaging enabled a close look at the interface between NPs in the NPNTs, showing effective coalescence and lattice continuation at both symmetric (Au−Au, Pd−Pd) and asymmetric (Au−Pd) interfaces. The coalescence occurs largely during the drying step prior to alumina membrane dissolution, but NP accumulation and initial coalescence must occur during the colloid flow through the membrane to obtain stable, multiwall NPNTs. While the use of pure Pd NP solutions does not lead to self-sustained NPNTs at room temperature due to absence of NP accumulation, stable 1:1 composite Au−Pd NPNTs were obtained using mixed NP solutions. The convenient preparation of composite NPNTs comprising different types of NP building blocks at predetermined ratios, promises extended use of such systems in various applications. Formation of intimate metal−metal interfaces by room-temperature coalescence of NPs may become a general approach to the synthesis of nanostructured materials under mild conditions using metal NPs as building blocks.

Acknowledgment. Support from the Minerva Foundation, Munich, and the Israel Science Foundation, is gratefully acknowledged. T. Sehayek was partially supported by a fellowship from the G. M. J. Schmidt Minerva Center on Supramolecular Architectures.

CM0501057